Electric Power Systems Research 188 (2020) 106570

Contents lists available at ScienceDirect

Electric Power Systems Research

journal homepage: www.elsevier.com/locate/epsr

Water distribution networks as flexible loads: A chance-constrained programming approach☆

Anna Stuhlmacher, Johanna L. Mathieu

Electrical Engineering and Computer Science University of Michigan, Ann Arbor, MI, USA

ARTICLE INFO

Keywords:
Chance-constrained optimization
Demand response
Distribution networks
Water networks

ABSTRACT

There is a greater need for flexibility in the power distribution network (PDN) due to increasing levels of renewable energy resources. Here, we consider using the water distribution network (WDN) as a flexible load. We formulate a chance-constrained multiperiod optimization problem to schedule water distribution pumps subject to WDN and PDN constraints while managing power demand forecast uncertainty. To do that, we develop a control policy that adjusts the WDN's operation when a PDN constraint violation is present. Since the resulting problem is nonconvex, we utilize approximation and relaxation techniques to transform the problem into a convex program and solve via the scenario approach. Through detailed case studies, we verify the performance of the control policy to ensure network constraints are satisfied despite uncertainty. We find that we can successfully schedule and control the WDN to provide flexibility to the PDN for many realistic water and power demand scenarios.

1. Introduction

There is increasing interest in optimization and control of coupled critical infrastructure systems to improve the systems' reliability, operational efficiency, and flexibility [1]. In this paper, we explore the intrinsic coupling between power distribution networks (PDNs) and water distribution networks (WDNs). These networks are spatially and temporally coupled through the power consumption of water pumps and storage capabilities of water tanks. PDNs are facing new challenges due to increasing levels of uncertainty from distributed energy resources like solar photovoltaics. WDNs are also experiencing issues such as increasing water demand and more energy intensive water treatment methods due to a shrinking fresh water supply [2]. Currently, the WDN is treated as an uncontrollable load on the electricity network. However, WDN supply pumps and storage tanks can be used as a source of flexibility, helping the PDN manage uncertainty that could lead to constraint violations.

The goal of this paper is to develop an approach to schedule WDN operation given WDN and PDN constraints. This problem is challenging since both networks include nonlinear and nonconvex constraints. Additionally, the PDN is subject to power demand uncertainty at buses with loads. To ensure that PDN voltage constraints are satisfied in the presence of uncertainty, we formulate the problem as a chance-constrained optimization problem and develop a real-time control policy that adjusts the water supply pumps' flow rates (and consequently power consumption) from the scheduled operation as a function of forecast error when voltage violations happen. The optimization problem determines both the WDN schedule and the control policy parameters.

There are significant bodies of work on optimal WDN operation and optimal PDN operation, see [3,4] for a review. There is also substantial work considering chance-constrained scheduling and control policies to handle uncertainties in power systems operation [5–7]. The number of papers that consider coordinating water and power networks are limited. In [8], water network operators respond to signals from the PDN to consume surplus energy. A water-power flow problem is developed in [9] and [10], where [9] implements a distributed solution algorithm and [10] proposes controlling irrigation systems to improve energy flexibility. In [11], the authors formulate an optimal water pumping problem to provide energy flexibility to the power transmission network.

To the best of our knowledge, optimal planning of a coupled WDN-PDN considering uncertainty has not been addressed except in our preliminary work [12]. In [12], we formulated a chance-constrained water pumping problem considering water demand uncertainty. In contrast, here, we consider power demand uncertainty, leading to a substantially different formulation. Moreover, [12] did not include storage tanks, PDN unbalance, or a multiperiod problem, all of which

☆ Submitted to the 21st Power Systems Computation Conference (PSCC 2020). This work was supported by the National Science Foundation Graduate Research Fellowship under Grant No. DGE 1256260.

E-mail addresses: akstuhl@umich.edu (A. Stuhlmacher), jlmath@umich.edu (J.L. Mathieu).

https://doi.org/10.1016/j.epsr.2020.106570
Received 3 October 2019; Received in revised form 27 March 2020; Accepted 20 July 2020
Available online 27 July 2020
0378-7796/ © 2020 Elsevier B.V. All rights reserved.

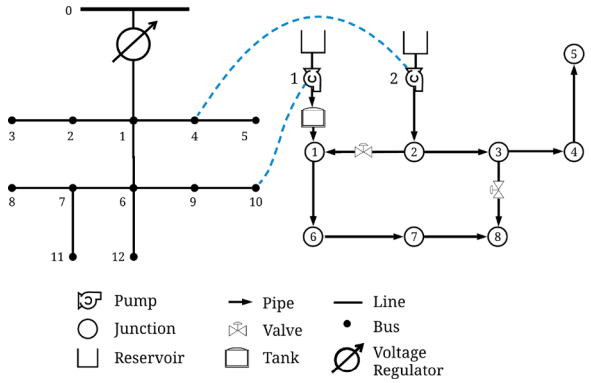

Fig. 1. Power (left) and water (right) distribution networks. The dashed lines show where the supply pumps are connected in the PDN.

we include here. Importantly, the control policy in [12] and related work [6,13] ensures supply and demand are balanced, whereas here the control policy determines corrective control actions that prevent constraint violations.

The contributions of this paper are the 1) design of a corrective control policy that responds to voltage constraint violations in real-time, 2) formulation of a chance-constrained optimization problem to choose a pumping schedule and control policy parameters considering power demand uncertainty, 3) reformulation of the problem into a chance-constrained convex quadratically constrained program using relaxations and approximations, 4) application of the scenario approach to solve the problem, and 5) assessment of the approach's performance through case studies.

2. Problem description

We consider a coupled WDN and PDN where the water pumps are loads on the PDN. See Fig. 1 for an example, which will be used in our case studies. In this section, we first describe how the pumps are scheduled and controlled to satisfy network constraints. Then, we detail the WDN and PDN models and apply relaxations to make the problem convex. We introduce uncertainty and develop the control policy used to modify pump operation in real-time. Last, we formulate the chance-constrained optimization problem.

2.1. Schedule and real-time control of WDN pumps

We solve for the WDN operational schedule (i.e., pump flow rates and tank levels) over a scheduling horizon subject to WDN and PDN constraints. We ensure that the network constraints are satisfied for the WDN's scheduled operation given forecasted water and power demands. The scheduling horizon is a set of discrete periods $t \in \mathcal{T}$ of duration ΔT.

Since the consumer power demand is uncertain, some forecast errors may cause PDN constraint violations when the WDN is operated as scheduled. To address this, we develop a control policy that adjusts the water supply pumps given power demand forecast errors. Not all power demand forecast errors require corrective action by the water pumps. In those cases, the pumps maintain their schedule. We assume that the WDN operator has full knowledge of the PDN and the WDN operator determines when to use the control policy based on the realized power demand forecast error at each bus and phase. Although this assumption may be impractical due to the present lack of communication systems and information sharing between WDNs and PDNs, this work provides us insights into the best possible solution without considering these challenges. Section 2.6 develops the control policy and Section 3 describes how we jointly optimize the schedule and control policy parameters.

2.2. Power distribution network model

We consider an unbalanced, radial PDN that includes a set of buses $\mathcal{K}$ to which consumers and water pumps are connected. We use the 3-phase, linearized, unbalanced model presented in [14]; however, other convex formulations could be used, such as [15]. In [14], the authors neglect the loss terms and assume that the voltage unbalance at each bus is small. Let $\Phi = \{a, b, c\}$ denote the three phases of the network. The linearized power flow model is [14]

$$\Upsilon_k^t = \Upsilon_n^t - \mathbb{M}_{kn}\mathbb{P}_n^t - \mathbb{N}_{kn}\mathbb{Q}_n^t \quad \forall\ k \in \mathcal{K}, t \in \mathcal{T}, \tag{1}$$

$$\mathbb{P}_k^t = \mathbf{P}_{L,k}^t + \sum_{n \in \mathcal{I}_k} \mathbb{P}_n^t \quad \forall\ k \in \mathcal{K}, t \in \mathcal{T}, \tag{2}$$

$$\mathbb{Q}_k^t = \mathbf{Q}_{L,k}^t + \sum_{n \in \mathcal{I}_k} \mathbb{Q}_n^t \quad \forall\ k \in \mathcal{K}, t \in \mathcal{T}, \tag{3}$$

where $\Upsilon_k^t := [\Upsilon_{k,\phi}^t]_{\phi \in \Phi}$ is a 3×1 vector of squared voltage magnitudes at bus k. Similarly, $\mathbb{P}_k^t$ and $\mathbb{Q}_k^t$ are 3×1 vectors of the real and reactive power flow entering bus k. The matrices $\mathbb{M}_{kn}$ and $\mathbb{N}_{kn}$ are formed from the line impedance matrices. The set $\mathcal{I}_k$ contains all buses that are directly downstream of bus k. The variables $\mathbf{P}_{L,k}^t := [P_{L,k,\phi}^t]_{\phi \in \Phi}$ and $\mathbf{Q}_{L,k}^t := [Q_{L,k,\phi}^t]_{\phi \in \Phi}$ are 3×1 vectors of the power demand at bus k, where the real and reactive power consumed at each phase is

$$P_{L,k,\phi}^t = \begin{cases} \rho_{k,\phi}^t + p_{e,\phi}^t, & \text{if pump } e \text{ connected to bus } k \\ \rho_{k,\phi}^t, & \text{otherwise} \end{cases}, \tag{4}$$

$$Q_{L,k,\phi}^t = \begin{cases} \zeta_{k,\phi}^t + q_{e,\phi}^t, & \text{if pump } e \text{ connected to bus } k \\ \zeta_{k,\phi}^t, & \text{otherwise} \end{cases}, \tag{5}$$

$\forall\ k \in \mathcal{K}, \phi \in \Phi, t \in \mathcal{T}$, where $\rho_{k,\phi}^t$ and $\zeta_{k,\phi}^t$ are the forecasted real and reactive net load, i.e., actual load minus distributed generation (which we assume is uncontrollable), at bus k and phase ϕ. The variables $p_{e,\phi}^t$ and are the real and reactive power demands of pump e on phase ϕ. We model the pumps as balanced three-phase constant power loads with real-to-reactive power ratios of μ_e.

The bus voltages are constrained

$$(V_k^{\min})^2 \le \Upsilon_{k,\phi}^t \le (V_k^{\max})^2 \quad \forall\ k \in \mathcal{K}, \phi \in \Phi, t \in \mathcal{T}, \tag{6}$$

where $V_k^{\min}$ and $V_k^{\max}$ are the lower and upper voltage limits at bus k. The voltage at the feeder head is regulated to V_{set}. We could also include apparent power flow constraints on the lines; however, since a voltage limit violation is more likely to occur first, we neglect them.

2.3. Water distribution network model

We consider an urban water distribution network. We assume the pipes' water flow does not change direction over the scheduling horizon. This assumption eliminates the need for binary variables when modelling pipes without pumps or valves. It is frequently used in the literature, e.g, in [8,9,16]. Note that pumps and valves only allow unidirectional water flow. As a result, we can represent the WDN as a directed graph $(\mathcal{N}, \mathcal{E})$ composed of a set of nodes $\mathcal{N}$ and a set of edges $\mathcal{E}$. Each node can be described as a junction $j \in \mathcal{J}$, reservoir $j \in \mathcal{R}$, or elevated storage tank $j \in \mathcal{S}$, i.e., $\mathcal{N} = \mathcal{J} \cup \mathcal{R} \cup \mathcal{S}$. The edges are pipes that connect nodes. A pipe may include a pump or a valve, $(\mathcal{P} \cup \mathcal{V}) \subseteq \mathcal{E}$. We assume a pump's on/off status is determined in advance of the scheduling problem. The WDN is described by the hydraulic head H_j^t at node j and the volumetric flow rate x_e^t through pipe e. Most urban WDNs are capable of operational control through their SCADA system [17]. We use the same hydraulic constraints as we did in [12] with several modifications: we include water storage tanks, we add time indexing so we can formulate a multiperiod problem, we approximate the pump characteristic curve with a linear function, and we use the Darcy-Weisbach method instead of the Hazen-Williams method

to model the pipe head loss. The last two modifications allow us transform the optimization problem into a convex program.

2.3.1. Nodes, $\mathcal{N}$

The hydraulic head H_j^t is composed of the pressure head and the elevation $\bar{h}_j$. The node constraints are

$$h_j^{\min} + \bar{h}_j \le H_j^t \le h_j^{\max} + \bar{h}_j \quad \forall\ j \in \mathcal{N}, t \in \mathcal{T}, \tag{7}$$

$$H_j^t = \bar{h}_j \quad \forall\ j \in \mathcal{R}, t \in \mathcal{T}, \tag{8}$$

$$\sum_{e \in \mathcal{E}} a_{je} x_e^t = d_j^t \quad \forall\ j \in \mathcal{J}, t \in \mathcal{T}, \tag{9}$$

$$H_{j,\text{out}}^t = H_{j,\text{out}}^{t-1} + \frac{\Delta T}{\gamma_j} \sum_{e \in \mathcal{E}} -a_{je} x_e^t \quad \forall\ j \in \mathcal{S}, t \in \mathcal{T}, \tag{10}$$

where $h_j^{\min}$ and $h_j^{\max}$ are the minimum and maximum pressure heads at node j, d_j^t is the water consumption at junction j, a_{je} is an element in the node-edge incidence matrix describing the connection of nodes and pipes in the network, and γ_j is the cross-sectional area of tank j. In (7), the hydraulic head at each node is bounded.

Reservoirs $\mathcal{R}$ are treated as an infinite source of water with a fixed pressure head. Therefore in (8), without loss of generality, the hydraulic head is set equal to the elevation head.

For junctions $\mathcal{J}$, (9) enforces that the sum of water flow rates entering and exiting a junction must equal the water consumption d_j^t at that junction.

For tanks $\mathcal{S}$, we use the same formulation as [8]. We model the hydraulic head going into and out of the tank, H_j^t and $H_{j,\text{out}}^t$, respectively, and assume the inlet of the water tank is located at the top of the tank. In (10), the hydraulic head at the tank outlet is calculated from the hydraulic head at the previous time period and the net inflow of the tank. To ensure that the tanks are not simply depleted at the end of the scheduling horizon, we constrain the final tank outlet head to be greater than or equal to the initial tank outlet head (i.e., $H_{j,\text{out}}^{t=|\mathcal{T}|} \ge H_{j,\text{out}}^{t=0}$). Similar to (7), the tank outlet head is physically bounded by the height and elevation of the tank.

2.3.2. Pipes, $\mathcal{E}$

The difference in head between the sending and receiving node, $\hat{H}_e^t = -\sum_{j \in \mathcal{N}} a_{je} H_j^t$, is equal to the pipe's head loss

$$\hat{H}_e^t = \begin{cases} -(m_e^0 + m_e^1 x_e^t) & \forall\ e \in \mathcal{P}, \quad (11a) \\ L_e^t & \forall\ e \in \mathcal{V}, \quad (11b) \\ k_e (x_e^t)^2 & \forall\ e \in \mathcal{E} \setminus (\mathcal{P} \cup \mathcal{V}), \quad (11c) \end{cases}$$

$\forall\ t \in \mathcal{T}$, where m_e^0 and m_e^1 are pump curve coefficients, and k_e is the resistance coefficient. The first case corresponds to pipes containing a fixed speed pump, the second to pipes containing a pressure reducing valve, and the third case to pipes without a pump or valve. For pipes with pressure reducing valves, the head loss $L_e^t \ge 0$ is a decision variable. While pumps are traditionally modeled with a quadratic pump characteristic curve, we neglect the quadratic term since its contribution is usually very small compared to the linear term [10]. The pumps' flow rates are bounded and nonnegative. The power consumption of a pump is a function of the head gain and flow rate

$$p_{e,\phi}^t = -\beta \hat{H}_e^t x_e^t \quad \forall\ e \in \mathcal{P}, \phi \in \Phi, t \in \mathcal{T}, \tag{12}$$

$$x_e^{\min} \le x_e^t \le x_e^{\max} \quad \forall\ e \in \mathcal{P}, t \in \mathcal{T}, \tag{13}$$

where $x_e^{\min}$ and $x_e^{\max}$ are pump e's flow rate limits, and β is a constant. Note that $p_{e,\phi}^t$ is a quadratic function of the pump's flow rate. The control policy described in Section 2.6 adjusts supply pumps drawing from reservoirs not in-line booster pumps that increase pressure head. To ensure that water supply meets water demand, our control policy formulation only applies to pumps bringing water into the network.

2.4. Deterministic problem

The deterministic problem minimizes the pumps' electricity cost given the forecasted power demand subject to WDN and PDN constraints

$$\begin{aligned} &\min_{\mathbf{x}} \textstyle\sum_{t \in \mathcal{T}} F^t(\mathbf{x}) \\ &\text{s.t. } (1) - (13); \end{aligned} \tag{D}$$

where the decision variables are $\mathbf{x} = \{x_e^t, H_j^t, H_{j,\text{out}}^t, L_e^t, \mathbb{Y}_k^t, \mathbb{P}_k^t, \mathbb{Q}_k^t, p_{e,\phi}^t\}$. The electricity consumption cost associated with the pump schedule at time t is

$$F^t(\mathbf{x}) := \sum_{e \in \mathcal{P}} \left(\pi_e^t \Delta T \sum_{\phi \in \Phi} p_{e,\phi}^t \right)$$

where π_e^t is the price of electricity at pump e and time t. We assume that the WDN is a price taker, i.e., the WDN's power consumption has no impact on electricity prices.

2.5. Convex relaxations

The WDN constraints are nonconvex due to the pipe head loss (11c) and the pump power consumption (12). Nonconvex problems are difficult to solve and so we use a convex relaxation, specifically, we take the convex hull of both quadratic constraints [10]. Equations (11c) and (12) become

$$\hat{H}_e^t \ge k_e (x_e^t)^2 \quad \forall\ e \in \mathcal{E} \setminus (\mathcal{P} \cup \mathcal{V}), t \in \mathcal{T}, \tag{14a}$$

$$\hat{H}_e^t \le b_e^0 + b_e^1 x_e^t \quad \forall\ e \in \mathcal{E} \setminus (\mathcal{P} \cup \mathcal{V}), t \in \mathcal{T}, \tag{14b}$$

$$p_{e,\phi}^t \ge -\beta \hat{H}_e^t x_e^t \quad \forall\ e \in \mathcal{P}, \phi \in \Phi, t \in \mathcal{T}, \tag{14c}$$

$$p_{e,\phi}^t \le -\beta (f_e^0 + f_e^1 x_e^t) \quad \forall\ e \in \mathcal{P}, \phi \in \Phi, t \in \mathcal{T}, \tag{14d}$$

where coefficients b_e^0 and b_e^1 provide an upper limit on head loss, and f_e^0 and f_e^1 provide an upper limit on pump power consumption. By replacing (11c) and (12) with (14a)-(14d), (D) becomes a convex quadratically constrained program. An advantage of implementing a convex hull relaxation is that extreme points of the convex hull are often in the original nonconvex set [10]. Since the cost of pumping is minimized in (D), the convex hull relaxation of (12) will be tight at the optimum whenever we want to reduce the pump power consumption, e.g., when there would be minimum voltage limit violations. In [10], the authors used a quasi-convex hull relaxation for (11c) (they did not assume flow direction) and found the relaxation was tight at the optimum in their case study.

2.6. Compensating power demand uncertainty

Next, we consider uncertainty in consumer power demand; we denote $\tilde{\rho}_{k,\phi}^t$ as the change in power demand from the forecast at bus k and phase ϕ. We formulate a control policy to adjust the pumps' flow rates from the scheduled operation as a function of the demand forecast errors. Since we do not want to use the control policy for uncertainty realizations that do not lead to constraint violations, we introduce an auxiliary binary variable $\tilde{s}^t \in \{0, 1\}$ that equals 1 when a minimum or maximum voltage limit violation would occur given the scheduled pump power consumption and the power demand uncertainty

realization at time t

$$\tilde{s}^t = \begin{cases} 0 \quad \text{if } (V_k^{\min})^2 \le \hat{\Psi}^t_{k,\phi}(\tilde{\boldsymbol{\rho}}^t, \mathbf{p}^t) \le (V_k^{\max})^2 \\ \quad \forall\ k \in \mathcal{K}, \phi \in \Phi \\ 1 \quad \text{otherwise} \end{cases} \tag{15}$$

where $\hat{\Psi}^t_{k,\phi}(\tilde{\boldsymbol{\rho}}^t, \mathbf{p}^t)$ is the voltage magnitude squared at bus k and phase ϕ given the power demand forecast errors $\tilde{\boldsymbol{\rho}}^t := [\tilde{\rho}^t_{k,\phi}]_{k\in\mathcal{K},\phi\in\Phi}$ and the scheduled pump power consumption $\mathbf{p}^t := [p^t_{e,\phi}]_{e\in\mathcal{P},\phi\in\Phi}$. Eqn. (15) can be reformulated

$$\hat{\Psi}^t_{k,\phi}(\tilde{\boldsymbol{\rho}}^t, \mathbf{p}^t) - (V_k^{\min})^2 \ge -M\tilde{s}^t \quad \forall\ k \in \mathcal{K}, \phi \in \Phi, \tag{16}$$

$$(V_k^{\max})^2 - \hat{\Psi}^t_{k,\phi}(\tilde{\boldsymbol{\rho}}^t, \mathbf{p}^t) \ge -M\tilde{s}^t \quad \forall\ k \in \mathcal{K}, \phi \in \Phi, \tag{17}$$

$\forall\ t \in \mathcal{T}$, where coefficient $M > 0$ is sufficiently large to ensure that when the left side of (16) or (17) is negative (i.e., a voltage violation occurs), the inequality is satisfied only when $\tilde{s}^t$ equals 1.

The control policy changes the pumps' flow rates from the schedule by

$$\tilde{x}^t_e = \tilde{s}^t \boldsymbol{C}^t_e \tilde{\boldsymbol{\rho}}^t \quad \forall\ e \in \mathcal{P}, t \in \mathcal{T}, \tag{18}$$

where $\tilde{x}^t_e$ is a random variable and $\boldsymbol{C}^t_e$ is a decision variable, specifically, a control policy parameter row vector that relates the power demand forecast error at bus k and phase ϕ to a change in pump e's flow rate. Despite the pump flow rate adjustments, the pumps and tanks must provide the same amount of water to the network. In our formulation, the tanks are not explicitly controlled, but compensate for the deviation between the supply and demand of water.

2.7. Chance-constrained optimization problem

We can write the stochastic counterparts of the deterministic equality constraints (1)-(5), (8)-(11b) and inequality constraints (6)-(7), (13)-(14d) using ($\tilde{\cdot}$) to denote deviations in variables due to power demand uncertainty. The complete set of stochastic constraints also includes the control policy constraints (16)-(18). The decision variables in the chance-constrained optimization problem are $\mathbf{x}_1 = \{x^t_e, H^t_j, H^t_{j,\text{out}}, L^t_e, \Psi^t_k, \mathbb{P}^t_k, \mathbb{Q}^t_k, p^t_{e,\phi}, \boldsymbol{C}^t_e\}$. Then the stochastic inequality constraints can be written compactly as $f(\mathbf{x}_1, \tilde{\boldsymbol{\rho}}) \le 0$ and transformed into a chance-constraint

$$\mathbb{P}(f(\mathbf{x}_1, \tilde{\boldsymbol{\rho}}) \le 0) \ge 1 - \epsilon, \tag{19}$$

where the constraints must jointly hold for a probability of at least $1 - \epsilon$, where ϵ is a user-selected violation level. Then, the chance-constrained problem to choose the scheduled WDN operation and control policy parameters over a planning horizon is

$$\begin{aligned} \min_{\mathbf{x}_1, J^t} \quad & \textstyle\sum_{t\in\mathcal{T}} F^t(\mathbf{x}_1) + gJ^t \\ \text{s.t.} \quad & (1) - (11b),\ (13) - (15b),\ (20), \\ & \|\boldsymbol{C}^t\|_F^2 \le J^t \quad \forall\ t \in \mathcal{T}, \end{aligned} \tag{MICP}$$

where gJ^t is the flexibility cost at time t and g is a weighting coefficient. The flexibility cost models the cost associated with adjusting pumps from their schedule in real-time (e.g., wear and tear on WDN components). To prevent control actions that are unnecessarily large, we minimize the magnitude of all parameters in the control policy. This is achieved by setting the variable J^t equal to the Frobenius norm squared of the control policy parameter matrix at time t. The resulting problem is a mixed-integer random convex program.

3. Solution approach

To solve the chance-constrained problem, we use the convex scenario approach [18], which solves the problem robustly for a set of scenarios. The number of scenarios required for probabilistic guarantees is a function of the user-selected maximum violation level ϵ and confidence level ψ. While there exist scenario approaches tailored to mixed integer random convex programs, e.g., [19,20], these methods require significantly more scenarios than the convex scenario approach in addition to requiring a more computationally intensive mixed-integer solver. To simplify the formulation, we remove the binary variable $\tilde{s}^t$ and apply the control policy to all scenarios, i.e., (16)-(18) in the chance constraint (19) is replaced with

$$\tilde{x}^t_e = \boldsymbol{C}^t_e \tilde{\boldsymbol{\rho}}^t \quad \forall\ e \in \mathcal{P}, t \in \mathcal{T}.$$

The simplified formulation, referred to as (CP), is a chance-constrained convex quadratically constrained program and so the convex scenario approach can be applied. The required number of scenarios N for user-selected ϵ and ψ is [18]

$$N \ge \frac{2}{\epsilon}\left(\ln\frac{1}{\psi} + \delta\right), \tag{20}$$

where δ is the number of decision variables. In Section 4.2.1, we verify the performance of (CP) against (MICP).

4. Case study

4.1. Set up

The WDN has 2 fixed speed pumps, 2 reservoirs, 2 pressure reducing valves, 8 junctions, and 11 pipes. We use the same WDN as [12] with some modifications. Specifically, we add a cylindrical storage tank upstream of junction 1, with a diameter of 25 m and a height of 30 m. The elevations at junction 6 and the reservoir upstream of pump 1 are 10 m, and the minimum pressure heads at junctions 7 and 8 are 20 m. The pump curve coefficients are $m^0_{e=1} = 75$ m and $m^1_{e=1} = 0.005\frac{\text{h}}{\text{m}^2}$ for pump 1, and $m^0_{e=2} = 90$ m and $m^1_{e=2} = 0.001\frac{\text{h}}{\text{m}^2}$ for pump 2. The pipe parameters from [21] are used to calculate the Darcy-Weisbach resistance coefficients k_e, see [22] for details. We set β equal to 2.322×10^{-3} kW/CMH·m.

For the PDN, the IEEE 13-bus feeder topology is used. Pumps 1 and 2 are connected to buses 10 and 4, respectively. The load and line parameters are from [23]. The distributed load along the line from bus 1 to 6 is placed at bus 1. The minimum and maximum voltage limits are 0.95 pu and 1.05 pu, respectively. We set the real-to-reactive pump power ratio to $\mu_e = 3$, i.e., a 0.949 lagging power factor. For each pump, there are 17 control policy parameters that correspond to each bus and phase where a load is present. We assume that all loads are wye-connected and constant power with a 0.9 lagging power factor. We ignore the voltage regulator and shunt admittance. We assume that the switch is closed and we do not model the transformer between buses 4 and 5. Also, we set the voltage at the feeder head equal to 4.16 kV line-to-neutral. The price of electricity is fixed for all periods at \$100/MWh. The weighting coefficient g is set to 1 $\$\cdot\text{kW}^2/\text{CMH}^2$, and we explore how changing g effects the solution.

We explore four cases, see Table 1. The cases vary in number of periods and demand multipliers, which are used to modify the nominal water and/or power demand uniformly across all junctions and/or buses. The entries of the demand multiplier vectors corresponds to

Table 1
Case Studies.

Case	# of Periods	Add Capacitive Load?	Demand Multipliers	
			Water	*Power*
A	1	No	1.00	1.50
B	1	Yes	1.00	1.50
C	3	No	[1.00,1.00,1.00]	[1.50,1.50,1.50]
D	3	No	[1.00,0.85,0.65]	[1.50,1.45,1.35]

Table 2
Number of Scenarios Needed for Scenario Approach.

User-selected Parameters		Number of Periods $\|\mathcal{T}\|$	
ϵ (%)	ψ (%)	1	3
10	10^{-3}	2,145	6,065
5	10^{-3}	4,289	12,128
3	10^{-3}	7,148	20,214

different periods. In Cases A, C, and D the PDN operates close to the minimum voltage limit. In Case B we add capacitive load, specifically, 500 kVAr at $k = 3$, $\phi = b$ and at $k = 6$, $\phi = \{a, b, c\}$ and 600 kVAr at $k = 10$, $\phi = b$, which increases the voltage and makes the system operate close to the maximum voltage limits.

Table 2 lists the number of scenarios needed for the case studies. We use a Gaussian probability distribution that is truncated 3 standard deviations from the mean to randomly generate independent power demand forecast error realizations for all buses and phases that have loads. The forecast error $\tilde{\rho}^t_{k,\phi}$ for bus k, phase ϕ, and time t has a mean of 0 and standard deviation of $\sigma \times \rho^t_{k,\phi}$ where σ is a percentage.

We solve the (MICP) and (CP) problems using the JuMP package in Julia with the GUROBI solver [24]. The optimization problems are solved on a 64-bit Intel i7 dual core CPU at 3.40 GHz and 16 GB of RAM.

4.2. Results

4.2.1. MICP versus CP

First, we explore the effect of removing the binary variables $\tilde{s}^t$ from our formulation. In the (CP) formulation, we apply the control policy to every scenario. Table 3 shows the results from (MICP) and (CP) for Case A with $N = 100$ randomly generated scenarios and $\sigma = 4\%$. Since g is 1, the flexibility cost is defined as $\sum_t \|\boldsymbol{C}^t\|_F^2$. The solutions are essentially identical but (CP) takes significantly less time. However, there are cases in which we would expect the formulations to produce different solutions, for example, those in which use of the control policy when the system does not need it would cause constraint violations. Further, different ways of representing the cost of flexibility could lead to different solutions from (CP) and (MICP).

4.2.2. Convex scenario approach

Next, we apply the convex scenario approach to (CP) for each of the cases in Table 1. The results are shown in Table 4 for each case, σ, and ϵ. We list the electricity and flexibility costs separately. As expected, when ϵ is reduced, the total cost increases. Additionally, there is less chance of constraint violations when σ is small resulting in smaller control policy parameters. For example, in Case D with $\sigma = 3\%$ and $\epsilon = 10\%$, it is cheaper to schedule the WDN operation to satisfy the PDN constraints for all scenarios than to schedule the WDN at a cheaper operation point and use the control policy to shift pumping in real-time. In Case D with $\sigma = 3\%$ and $\epsilon = 5\%$ or 3%, the flexibility costs round to zero but are non-zero because a small amount of flexibility is needed to manage the additional scenarios.

The solver computation times are reported in Table 4. As the number of periods increases, there is a significant increase in time and memory. We attempted a scheduling problem with 6 periods; however, for violation levels smaller than $\epsilon = 10\%$, we had memory storage errors. This problem could partially be addressed with more efficient coding and/or using methods to speed up the solver. We are currently exploring ways to make the approach scalable to large networks and longer time horizons.

Table 3
Comparison of MICP and CP solver solutions.

Problem	Time (s)	Total Cost	Electricity Cost ($)	Flexibility Cost
(MICP)	74,488.43	25.805	25.071	0.734
(CP)	0.27	25.805	25.069	0.736

Table 4
Scenario approach results.

Case	σ (%)	ϵ (%)	Electricity Cost ($)	Flexibility Cost	Comp. Time (s)	Empirical Violation Probability (%)	
						General	*Selected*
A	3	10	24.03	0.288	18.39	0.035	0.035
		5	24.04	0.287	40.46	0.035	0.035
		3	24.23	0.802	54.64	0.015	0.015
	4	10	25.67	1.146	15.15	0.119	0.101
		5	25.67	1.146	30.04	0.119	0.101
		3	25.04	3.000	46.23	0.019	0.019
B	3	10	23.73	0.023	22.94	0.484	0.000
		5	23.75	0.058	32.83	0.111	0.000
		3	23.75	0.058	68.43	0.091	0.000
	4	10	23.95	0.402	16.69	0.290	0.039
		5	23.97	0.569	38.28	0.209	0.044
		3	24.00	0.935	72.81	0.186	0.030
	5	10	24.07	1.257	19.53	0.512	0.321
		5	24.32	2.051	36.20	0.340	0.242
		3	25.01	4.271	59.70	0.196	0.127
C	3	10	71.75	1.162	654.82	0.123	0.123
		5	72.18	1.520	1717.05	0.082	0.082
		3	73.04	2.337	3200.44	0.029	0.029
	4	10	76.73	3.234	667.88	0.246	0.229
		5	76.06	5.301	1525.91	0.139	0.137
		3	75.00	9.356	2299.50	0.055	0.055
D	3	10	59.18	0.000	581.89	0.069	0.025
		5	59.19	0.000	1820.04	0.004	0.004
		3	59.19	0.000	2641.91	0.004	0.004
	4	10	59.24	0.002	749.27	0.055	0.047
		5	59.33	0.007	1330.84	0.034	0.029
		3	59.46	0.321	3021.37	0.010	0.009

Table 4 also includes the empirical violation probabilities. For each case, σ, and ϵ, we test the optimal schedule and control policy parameters on 100,000 independent randomly generated scenarios and report the percent of scenarios for which there is at least one constraint violation. We compute the empirical violation probabilities two ways: *general* refers to the violation probability computed for the case in which the control policy is applied to all scenarios and *selected* refers to the violation probability computed for the case in which the control policy is applied only when needed (i.e., there is a voltage constraint violation). Therefore, the *general* violation probabilities correspond to the problem actually solved with the convex scenario approach, whereas the *selected* violation probabilities correspond to the more realistic case. Note that the *general* violation probability is always greater than or equal to its corresponding *selected* violation probability since applying the control policy when it is not needed can result in a constraint violation. Also note that all empirical violation probabilities are significantly less than the user-selected violation level, which is typical for problems solved with the scenario approach [25]. If we had chosen a more atypical probability distribution from which to draw scenarios, we would have achieved less conservative results.

Next, we investigate how the location of the forecast error impacts the control policy parameters. Fig. 2 shows the relative magnitude of the negative and positive control policy parameters associated with each bus and phase in Case A. We show the positive and negative control policy parameters separately since they serve different purposes. A negative control policy parameter reduces a pump's flow rate and power consumption given an increase in load. Therefore, the negative control policy parameters serve to correct voltage limit violations and the positive control policy parameters serve to balance water supply and demand. The magnitudes of the negative control policy

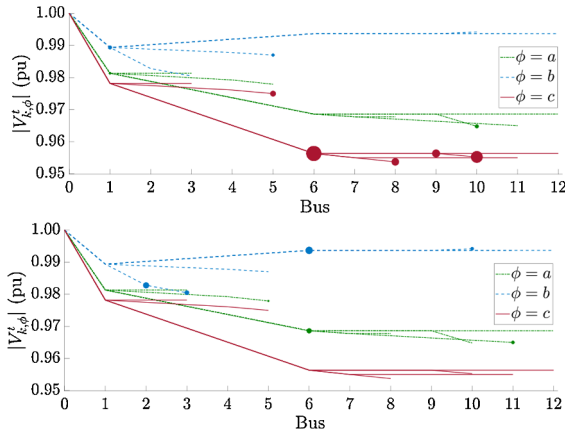

Fig. 2. 3-phase PDN voltage profile for the optimal scheduled WDN operation in Case A ($\sigma = 4\%$, $\epsilon = 3\%$). The marker size at each bus and phase is scaled according to the magnitude of the pump's control policy parameters, where the top plot shows the magnitude of the negative control policy parameters and the bottom plot shows the magnitude of the positive control policy parameters. The magnitudes of the negative/positive control policy parameters show which buses and phases are most/least likely to cause voltage limit violations.

parameters show which buses/phases are most likely to cause voltage limit violations, and the magnitudes of the positive control policy parameters show which buses/phases are least likely to cause voltage limit violations. The PDN is close to the minimum voltage limit on phase *c* and we observe that the negative control policy parameters are largest on phase *c*. In Case B (not shown), phase *b* is close to the maximum voltage limit and phase *a* is close to the minimum voltage limit. The negative control policy parameters are largest on phase *b*, followed by those on phase *a*.

Fig. 3 shows how considering uncertainty affects the optimal pump and tank schedule, specifically, it shows the optimal decisions from the scenario approach versus the deterministic approach for Cases C and D. The scenario approach decisions vary more over the scheduling horizon since they are co-optimized with the control policy parameters. The edges of the light and dark blue bands show the largest and average pump and tank adjustments from the scenario approach's schedule made by the control policy in the presence of a voltage violation (in computing the largest/average we exclude adjustments that violate constraints). In this case, the bands extend downward from the scheduled operation since the bus voltages are near the minimum voltage limit and the control policy is working to raise the voltage levels by

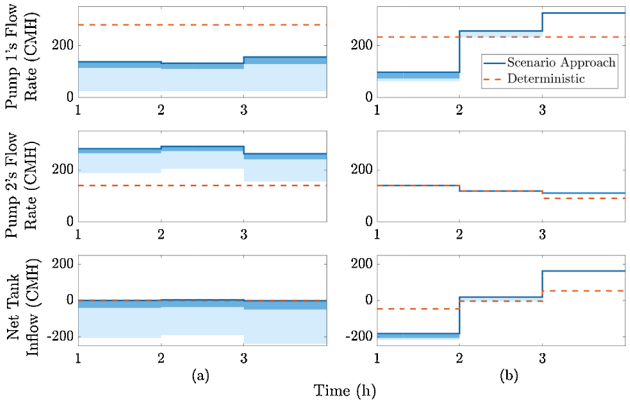

Fig. 3. Pump and tank schedules for the scenario approach versus the deterministic approach for (a) Case C, $\sigma = 4\%$, $\epsilon = 3\%$, and (b) Case D, $\sigma = 4\%$, $\epsilon = 3\%$. The edges of light/dark blue bands show the largest/average pump and tank adjustments from the scenario approach's schedule made by the control policy. (For interpretation of the references to color in this figure legend, the reader is referred to the web version of this article.)

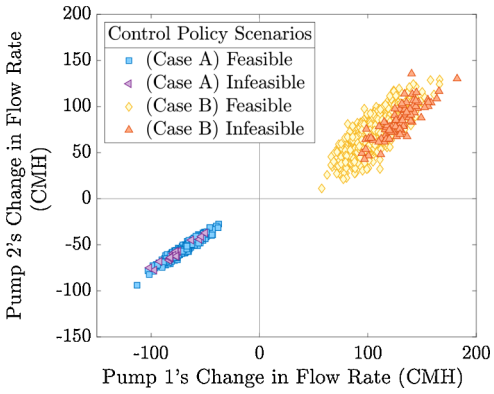

Fig. 4. Change in pump flow rates for Case A ($\sigma = 4\%$, $\epsilon = 3\%$) and Case B ($\sigma = 5\%$, $\epsilon = 3\%$) for scenarios in the test set requiring the control policy.

decreasing pumping. For Case D, the bands are smaller since the pump and tank schedule is more conservative and less real-time control is required. Specifically, pumping is shifted to periods 2 and 3 when there is less power demand.

Fig. 4 shows the pump adjustments made by the control policy in the presence of a voltage violation for Cases A and B. For each scenario, we indicate whether the network constraints were satisfied after implementing the pump adjustment. The scenarios for Case A are in the lower right quadrant because the network experiences minimum voltage limit violations. Consequently, the pump power consumption is reduced in order to raise the voltage levels. The scenarios for Case B are in the upper right quadrant because the network experiences maximum voltage limit violations and pump power consumption needs to increase.

Fig. 5 shows how the control policy corrects voltage deviations. For Cases A and B, we compare the voltage profile associated with a power demand scenario before and after the control policy adjusts the pump operation. The voltage profile associated with the schedule is outside of the voltage limits. Once the pumps are adjusted, the voltage profile is within the voltage limits. The insets zoom in on the critical voltages.

The coefficient *g* determines the relative cost of the schedule versus the cost of the real-time control actions. Fig. 6 shows how the scheduled electricity cost and flexibility change as we vary *g*. The best choice of *g* would be a function of the real cost to WDN operators of changing pump schedules, and is a topic for future research.

Finally, we evaluate our WDN relaxations and PDN approximations. We find that, in our case study, the pump power consumption

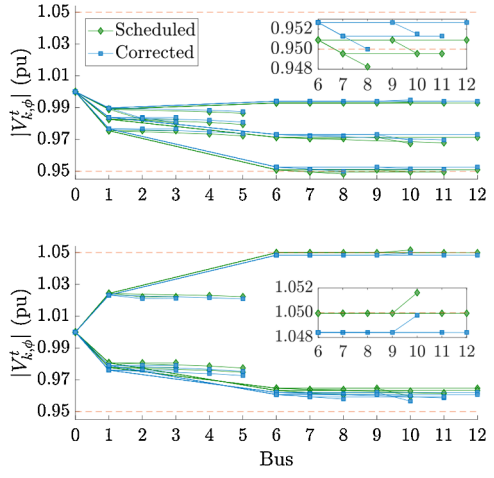

Fig. 5. PDN voltage profile for a power demand scenario before (Scheduled) and after (Corrected) use of the control policy. Top: Case A ($\sigma = 4\%$, $\epsilon = 3\%$). Bottom: Case B ($\sigma = 5\%$, $\epsilon = 3\%$).

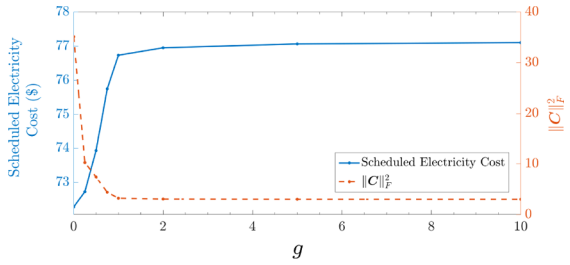

Fig. 6. Comparison of scheduled electricity cost and flexibility as the weighting coefficient g varies, for Case C, $\sigma = 4\%$, $\epsilon = 10\%$.

relaxation is tight for cases close to the minimum voltage limit, i.e., Cases A, C, and D. In Case B, the pump power consumption is increased above the convex hull's lower bound in order to fix the overvoltages. Additionally, the pipe head loss relaxation is not tight; however, we are able to recover the actual heads from the pump flow rates. In [26], the authors prove uniqueness of the water flow equations for several network configurations. Given the pump flow rates, the authors recover the head values by solving a convex energy minimization problem. While their proof does not extend to meshed networks that contain valves, our case study solutions appear unique and optimal when we test many solver initialization points. Additionally, the heads found in the relaxed problem are always less than or equal to the recovered heads. Since we are primarily concerned with head lower limits, we can be certain that the recovered heads are feasible. Lastly, we find that the voltage difference between the linearized unbalanced power flow and the ac power flow is minimal, e.g., for Case B, $\sigma = 5\%$, $\epsilon = 3\%$, the largest difference is 0.34%.

5. Conclusion

In this paper, we explored using the WDN to provide load flexibility for the PDN. We formulated a chance-constrained water pumping problem subject to WDN and PDN constraints, and including power demand uncertainty. We utilized corrective control to adjust the pumps' flow rates to respond to PDN demand uncertainty in real-time. We applied the convex scenario approach and found that we were able to successfully schedule and control the pumps to respond to voltage violations in the PDN. A drawback to this approach is the time needed to solve this problem when scaling to larger networks and longer optimization horizons. In future work, we plan to improve the scalability of this approach through use of distributed optimization methods. Additionally, we will consider multiple sources of uncertainty.

Declaration of Competing Interest

The authors declare that they do not have any financial or non-financial conflict of interests

References

[1] E. Dall'Anese, P. Mancarella, A. Monti, Unlocking flexibility: integrated optimization and control of multienergy systems, IEEE Power Energy Mag. 15 (1) (2017) 43–52.
[2] International Energy Agency, World energy outlook 2016, Paris, (2016).
[3] H. Mala-Jetmarova, N. Sultanova, D. Savic, Lost in optimisation of water distribution systems? a literature review of system operation, Environ. Modell. Software 93 (2017) 209–254.
[4] D.K. Molzahn, I.A. Hiskens, A survey of relaxations and approximations of the power flow equations, Found. Trend. Electr. Energy Syst. (2019).
[5] E. Dall'Anese, K. Baker, T. Summers, Chance-constrained ac optimal power flow for distribution systems with renewables, IEEE Trans. Power Syst. 32 (5) (2017) 3427–3438.
[6] M. Vrakopoulou, B. Li, J.L. Mathieu, Chance constrained reserve scheduling using uncertain controllable loads part I: formulation and scenario-based analysis, IEEE Trans. Smart Grid 10 (2) (2019) 1608–1617.
[7] L. Roald, S. Misra, T. Krause, G. Andersson, Corrective control to handle forecast uncertainty: a chance constrained optimal power flow, IEEE Trans. Power Syst. 32 (2) (2017) 1626–1637.
[8] D. Fooladivanda, A.D. Dominguez-Garcia, P. Sauer, Utilization of water supply networks for harvesting renewable energy, IEEE Trans. Control Netw. Syst. 6 (2) (2019) 763–774.
[9] A. Zamzam, E. Dall'Anese, C. Zhao, J. Taylor, N. Sidiropoulos, Optimal water-power flow problem: formulation and distributed optimal solution, IEEE Trans. Control Netw. Syst. 6 (1) (2019) 37–47.
[10] Q. Li, S. Yu, A. Al-Sumaiti, K. Turitsyn, Micro water-energy nexus: optimal demand-side management and quasi-convex hull relaxation, IEEE Trans. Control Netw. Syst. 6 (4) (2019) 1313–1322.
[11] K. Oikonomou, M. Parvania, Optimal coordination of water distribution energy flexibility with power systems operation, IEEE Trans. Smart Grid 10 (1) (2019) 1101–1110.
[12] A. Stuhlmacher, J.L. Mathieu, Chance-constrained water pumping to support the power distribution network, North American Power Symposium, (2019).
[13] L. Roald, G. Andersson, S. Misra, M. Chertkov, S. Backhaus, Optimal power flow with wind power control and limited expected risk of overloads, Power Systems Computation Conference, (2016).
[14] D.B. Arnold, M. Sankur, R. Dobbe, K. Brady, D.S. Callaway, A. Von Meier, Optimal dispatch of reactive power for voltage regulation and balancing in unbalanced distribution systems, IEEE Power and Energy Society General Meeting, (2016).
[15] L. Gan, S.H. Low, Convex relaxations and linear approximation for optimal power flow in multiphase radial networks, Power Systems Computation Conference, (2014).
[16] D. Fooladivanda, J.A. Taylor, Energy-optimal pump scheduling and water flow, IEEE Trans. Control Netw. Syst. 5 (3) (2018) 1016–1026.
[17] D. Denig-Chakroff, Reducing electricity used for water production: questions state commissions should ask regulated utilities, Technical Report, Water Research and Policy, 2008.
[18] M.C. Campi, S. Garatti, M. Prandini, The scenario approach for systems and control design, Annu. Rev. Control 33 (2) (2009) 149–157.
[19] S. Grammatico, X. Zhang, K. Margellos, P. Goulart, J. Lygeros, A scenario approach for non-convex control design, IEEE Trans. Autom. Control 61 (2) (2016) 334–345.
[20] M.C. Campi, S. Garatti, F.A. Ramponi, A general scenario theory for nonconvex optimization and decision making, IEEE Trans. Autom. Control 63 (12) (2018) 4067–4078.
[21] D. Cohen, U. Shamir, G. Sinai, Optimal operation of multi-quality water supply systems-II: the Q-H model, Eng. Opt. 32 (6) (2000) 687–719.
[22] P.R. Bhave, R. Gupta, Analysis of water distribution networks, Alpha Science International Ltd., Oxford, U.K., 2006.
[23] W.H. Kersting, Radial distribution test feeders, IEEE Power Eng. Soc. Winter Meet. 2 (2001), pp. 908–912.
[24] Gurobi Optimization, LLC, Gurobi Optimizer Reference Manual, 2019, http://www.gurobi.com.
[25] M. Vrakopoulou, K. Margellos, J. Lygeros, G. Andersson, A probabilistic framework for reserve scheduling and N− 1 security assessment of systems with high wind power penetration, IEEE Trans. Power Syst. 28 (4) (2013) 3885–3896.
[26] M. Singh, V. Kekatos, On the flow problem in water distribution networks: Uniqueness and solvers (2019). ArXiv:1901.03676.